韓國海洋工學會誌 第11卷 第3號, pp.107~115, 1997. 8

◉ 論 文

Responses of a Roll-Pitch Coupled Nonlinear System to the Primary Resonance of the Roll Mode

Il-Geun Oh*

(97년 7월 3일 접수)

횡동요 모드와 주공진 된 횡-종동요연성 비선형계의 응답

오 일 근*

Key Words : Nonlinear Dynamic Responses (비선형 동적 응답), Two-to-One Internal Resonance (2:1 내부공진), Stability Analysis (안정성 해석), Linear Plus-Quadratic Damping Model (선형 및 제곱형 감쇄 모형), Primary Resonance (주공진), Method of Multiple Scales (다중척도법)

초 록

비선형 동력학계로 모델링된 부유수송체의 동적응답을 조사하고 그 운동의 안정성을 해석하였다. 종동요 모우드의 고유주파수가 횡동요 모우드의 고유주파수의 두 배가 되는, 즉, 2:1 내부공진 혹은 자기계수공진인 조건 하에서, 이 부유수송체는 한 운동 모우드의 직접가진에 의해 간접가진된 다른 모우드가 대진폭 응답을 보일 수 있음을 밝혔다. 또한, 종동요 모우드의 감쇠력은 비교적 넓은 범위의 운동에 대해 선형적인데 반해, 횡동요 모우드의 감쇠력은 점성의 영향이 대단히 커서 비선형성이 대단히 강한 것으로 알려져 왔다. 이 문제를 수학적으로 모델링하기 위하여, 종동요 모우드의 운동방정식에는 선형 감쇠력만을 사용하는 한편, 횡동요 모우드의 운동방정식에는 선형 및 제곱형의 합의 형태인 감쇠력 모형을 사용하였다. 다중척도법을 사용하여 이 두 가지 운동 모우드의 주기적 응답 및 그의 안정성에 미치는 제곱형 비선형 횡동요 감쇠력의 영향을 밝혔다. 조우주기가 횡동요 모우드의 고유주기와 근사한 경우에 대하여 이 비선형계의 응답을 구하고 주파수-응답 곡선으로 나타내었다.

1. INTRODUCTION

One must understand the complicated dynamics of a vessel moving in a general environment to design more comfortable and safe vessels since the extent of the motion that a marine vehicle may experience has important consequences on its safety, operability, and economical aspects.

Loss of stability due to excessive motions,

* 한국철도연구원

such as heavy rolling, can happen through the energy transfer between the modes of motion if nonlinearities are present and various resonances of the internal, external, or parametric type occur. The present research is concerned with the dynamic stability and excessive motion of a vessel in the presence of two-to-one internal or autoparametric resonance in which the natural frequency in pitch is twice that in roll.

The significance of internal resonance has been recognized recently in many mechanical and elastic systems. There are a number of references dealing with physical two-degree-of-freedom systems. Among others, Nayfeh and Mook discussed problems involving the forced responses of ships, robots, elastic pendulums, beams and plates under static loadings, composite plates, arches, shells, and the sloshing of liquid gasoline in the fuel container of an airplane.[1] When these systems possess internal (or autoparametric) resonances, which may occur if the natural frequencies of the system are commensurate, their responses may exhibit extraordinarily complicated behaviors, which cannot be explained by linear formulations.

Interestingly, two-to-one autoparametric or internal resonances may strongly influence the dynamic behavior and stability of vessels.[1] A strong coupling of the involved modes of motion produced by internal or autoparametric resonance was first observed by Froude in 1863. He observed that a vessel whose linear undamped natural frequency in pitch is twice that in roll has undesirable seakeeping characteristics.[2] This observation was a manifestation of the two-to-one internal resonance whose significance cannot be determined using linearized equations.[3),4)]

For a century after Froude, however, no further research on this phenomenon was pursued. In 1959, Paulling and Rosenberg studied the coupled heave-roll motion of a vessel using a set of nonlinear ordinary-differential equations.[5] They simplified the equations of motion and obtained a single roll equation having the form of a simple linear Mathieu equation which contains a time-varying coefficient due to a simple harmonic motion of the heave mode. This study has a principal shortcoming; due to the lack of consideration for damping and nonlinear coupling terms, the analytical model was not capable of yielding realistic results.

To explain Froude's observation, Nayfeh, Mook, and Marshall modeled the ship motion by two nonlinearly coupled equations involving the pitch and roll modes; they included the dependence of the pitching moment on the roll orientation.[6] They clearly showed the significance of the frequency ratio in causing undesirable roll behaviors, such as the "saturation" phenomenon. They offered an explanation of the observations of Froude.

In the present paper, we use a linear-plus-quadratic damping model for the roll motion. The linear-plus-quadratic damping model has long been recognized by investigators to describe closely the dissipation of energy in the roll mode. However, it was not used so far because of some analytical difficulties. We obtain various complicated responses, which are common features of the nonlinear dynamics of many mechanical and elastic systems. These responses include supercritical and subcritical instabilities, periodic motions, and coexistence of multiple solutions and associated jumps. Such phenomena can never be addressed by the linear approach because it is incapable of representing not only the strong nonlinear interaction between the two modes but also the effect of the viscous damping in the roll mode.

2. EQUATIONS OF MOTION

We consider the response of a ship that is

restricted to pitch and roll to a regular wave. We assume that the ship is laterally symmetric. We use the right-handed coordinate systems : a body-fixed coordinate system $oxyz$ such that its origin o is at the center of mass. The x-axis is positive toward the bow, the y-axis is positive toward starboard, and the z-axis is positive downward. The orientation of the ship with respect to an inertial frame $OXYZ$ is defined by the Euler angles $\varnothing$ and θ as follows: θ is a pitch rotation about the original y-axis, and $\varnothing$ is a roll rotation about the new x-axis. The components p and q of the angular velocity about the x- and y-axes are related to $\varnothing, \theta, \dot{\varnothing}$, and $\dot{\theta}$ by

$$p=\dot{\varnothing} \quad \text{and} \quad q=\dot{\theta}\cos\varnothing \tag{1}$$

The equations of motion can be written as

$$I_{xx}\dot{p}-I_{xz}\dot{p}q=K+K_0\cos\Omega t \tag{2}$$

$$I_{yy}\dot{q}+I_{xz}\dot{p}^2=M+M_0\cos(\Omega t+\tau) \tag{3}$$

where I_{xx}, I_{yy}, and I_{xz} are the moments and product of inertia, Ω is the encounter frequency, K_0 and M_0 are the amplitudes of the moments produced by the waves, and τ is a phase; they are assumed constants. We assume that the hydrodynamic moments K and M are analytic functions of $\varnothing$ and θ and their derivatives. Following Nayfeh, Mook, and Marshall and including a quadratic damping term in the roll equation, we obtain

$$\begin{aligned}\ddot{\varnothing}+\omega_1^2\varnothing &= \varepsilon[-2\mu_1\dot{\varnothing}-\mu_3\dot{\varnothing}\,|\,\dot{\varnothing}\,| \\ &\quad +\delta_1\varnothing\theta+\delta_2\varnothing\ddot{\theta} \\ &\quad +\delta_3\theta\ddot{\varnothing}+\delta_4\dot{\varnothing}\dot{\theta}+F_1\cos\Omega t\,]\end{aligned} \tag{4}$$

$$\begin{aligned}\ddot{\theta}+\omega_2^2\theta &= \varepsilon[-2\mu_2\dot{\theta}+\alpha_1\varnothing^2+\alpha_2\varnothing\ddot{\varnothing} \\ &\quad +\alpha_3\theta^2+\alpha_4\theta\ddot{\theta}+\alpha_5\dot{\varnothing}^2+\alpha_6\dot{\theta}^2 \\ &\quad +F_2\cos(\Omega t+\tau)]\end{aligned} \tag{5}$$

where ε is a small dimensionless parameter that is introduced as a bookkeeping device in the perturbation analysis that follows.[6]

3. METHOD OF MULTIPLE SCALES

We use the method of multiple scales to determine a first-order approximation to the solutions of equations (4) and (5).[7,8] We let

$$\varnothing(t;\varepsilon)=\varnothing_0(T_0,T_1)+\varepsilon\varnothing_1(T_0,T_1)+\ldots \tag{6}$$

$$\theta(t;\varepsilon)=\theta_0(T_0,T_1)+\varepsilon\theta_1(T_0,T_1)+\ldots \tag{7}$$

where $T_0=t$ is a fast time scale, characterizing motions on the scales ω_1 and Ω ; and $T_1=\varepsilon t$ is a slow time scale, characterizing the modulation of the amplitudes and phases of the motion. In terms of T_0 and T_1, the time derivatives are transformed into

$$\frac{d}{dt}=D_0+\varepsilon D_1+\ldots \tag{8}$$

and $$\frac{d^2}{dt^2}=D_0^2+2\varepsilon D_0D_1+\ldots$$

where $D_n=\partial/\partial T_n$.

Substituting equations (6)-(8) into equations (4) and (5) and equating coefficients of like powers of ε, we obtain

$O(\varepsilon^0)$:

$$D_0^2\varnothing_0+\omega_1^2\varnothing_0=0 \tag{9}$$

$$D_0^2\theta_0+\omega_2^2\theta_0=0 \tag{10}$$

$O(\varepsilon)$:

$$\begin{aligned}D_0^2\varnothing_1+\omega_1^2\varnothing_1 &= -2D_0D_1\varnothing_0-2\mu_1D_0\varnothing_0 \\ &\quad -\mu_3D_0\varnothing_0\,|\,D_0\varnothing_0\,|+\delta_1\varnothing_0\theta_0 \\ &\quad +\delta_2\varnothing_0D_0^2\theta_0+\delta_3\theta_0D_0^2\varnothing_0 \\ &\quad +\delta_4D_0\varnothing_0\theta_0+F_1\cos\Omega T_0\end{aligned} \tag{11}$$

$$D_0^2\theta_1 + \omega_2^2\theta_1 = -2D_0D_1\theta_0 - 2\mu_2 D_0\theta_0 + \alpha_1\varnothing_0^2 + \alpha_2\varnothing_0 D_0^2\varnothing_0 + \alpha_3\theta_0^2 + \alpha_4\theta_0 D_0^2\theta_0 + \alpha_5(D_0\varnothing_0)^2 + \alpha_6(D_0\theta_0)^2 + F_2\cos(\Omega T_0 + \tau) \quad (12)$$

The solutions of equations (9) and (10) can be expressed as

$$\varnothing_0 = A_1(T_1)e^{i\omega_1 T_0} + \overline{A_1}(T_1)e^{-i\omega_1 T_0} \quad (13)$$

$$\theta_0 = A_2(T_1)e^{i\omega_2 T_0} + \overline{A_2}(T_1)e^{-i\omega_2 T_0} \quad (14)$$

where A_1 and A_2 are unknown functions at this level of approximation. They are determined by imposing the solvability conditions at the next level of approximation. Alternatively, the solutions of equations (13) and (14) can be expressed as

$$\varnothing_0 = a_1(T_1)\cos[\omega_1 T_0 + \beta_1(T_1)] \quad (15)$$

$$\theta_0 = a_2(T_1)\cos[\omega_2 T_0 + \beta_2(T_1)] \quad (16)$$

where the a_n and β_n are the amplitudes and phases of the roll and pitch modes. Comparing equations (13) and (14) with equations (15) and (16), we conclude that

$$A_n(T_1) = \frac{1}{2}a_n(T_1)e^{i\beta_n(T_1)} \quad (17)$$

Substituting equations (13) and (14) into equations (11) and (12) yields

$$D_0^2\varnothing_1 + \omega_1^2\varnothing_1 = -2i\omega_1(A_1' + \mu_1 A_1)e^{i\omega_1 T_0} + (\delta_1 - \omega_2^2\delta_2 - \omega_1^2\delta_3 - \omega_1\omega_2\delta_1)A_2A_1e^{i(\omega_2+\omega_1)T_0} + (\delta_1 - \omega_2^2\delta_2 - \omega_1^2\delta_3 + \omega_1\omega_2\delta_4)A_2\overline{A_1}e^{i(\omega_2-\omega_1)T_0} + \frac{1}{2}F_1e^{i\Omega T_0} + cc + f[i\omega_1 A_1e^{i\omega_1 T_0} - i\omega_1\overline{A_1}e^{-i\omega_1 T_0}] \quad (18)$$

$$D_0^2\theta_1 + \omega_2^2\theta_1 = -2i\omega_2(A_2' + \mu_2 A_2)e^{i\omega_2 T_0} + (\alpha_1 - \omega_1^2\alpha_2 - \omega_1^2\alpha_5)A_1^2e^{2i\omega_1 T_0} + (\alpha_3 - \omega_2^2\alpha_4 - \omega_2^2\alpha_6)A_2^2e^{2i\omega_2 T_0} + (\alpha_1 - \omega_1^2\alpha_2 + \omega_1^2\alpha_5)A_1\overline{A_1} + (\alpha_3 - \omega_2^2\alpha_4 + \omega_2^2\alpha_6)A_2\overline{A_2} + \frac{1}{2}F_2e^{i(\Omega T_0+\tau)} + cc \quad (19)$$

where the prime indicates the derivative with respect to T_1, $\overline{A_n}$ is the complex conjugate of A_n, and the function f accounts for the term $-\mu_3 D_0\varnothing_0|D_0\varnothing_0|$. Depending on the functions A_n, particular solutions of equations (18) and (19) contain terms proportional to $T_0e^{\pm i\omega_n T_0}$ (*i.e.*, secular terms). They also contain small-divisor terms if $\Omega \approx \omega_1$ or $\Omega \approx \omega_2$ (*i.e.*, primary resonances of the pitch or roll mode) and/or if $\omega_2 \approx 2\omega_1$ (the frequency of pitch mode is approximately twice that of roll mode; *i.e.*, two-to-one internal or autoparametric resonance).

To eliminate the secular and small-divisor terms, we first expand $f(D_0\varnothing_0)$ in a Fourier series as

$$f = \sum_{n=-\infty}^{\infty} f_n(A_1, \overline{A_1})e^{in\omega_1 T_0} \quad (20)$$

where

$$f_n(A_1, \overline{A_1}) = \frac{\omega_1}{2\pi}\int_0^{2\pi/\omega_1} fe^{-in\omega_1 T_0}dT_0 \quad (21)$$

Consequently, the component of f that produces a secular term is

$$\frac{\omega_1}{2\pi}\int_0^{2\pi/\omega_1} fe^{-i\omega_1 T_0}dT_0 . \quad (22)$$

We analyze the case of primary resonance of the roll mode in the next Section.

4. ANALYSIS

4.1 Modulation Equations

To express the nearness of the resonances for the case of primary resonance of the roll mode, we introduce two detuning parameters, σ_1 and σ_2, defined $\Omega = \omega_1 + \varepsilon\sigma_2$ and $\omega_2 = 2\omega_1 + \varepsilon\sigma_1$. Then, we have

$$\begin{aligned}\Omega T_o &= \omega_1 T_O + \sigma_2 T_1 \\ \omega_2 T_o &= 2\omega_1 T_o + \sigma_1 T_1\end{aligned} \tag{23}$$

Using equations (23) and (22) to eliminate the terms that produce secular terms from equations (18) and (19), we obtain

$$2i(A_1' + \mu_1 A_1) - 4\Lambda_1 A_2 \overline{A_1} e^{i\sigma_1 T_1} - f_1 e^{i\sigma_2 T_1} - \frac{1}{2\pi}\int_0^{2\pi/\omega_1} f e^{-i\omega_1 T_O} dT_O = 0 , \tag{24}$$

$$2i(A_2' + \mu_2 A_2) - 4\Lambda_2 A_1^2 e^{-i\sigma_1 T_1} = 0 , \tag{25}$$

where

$$4\omega_1\Lambda_1 = \delta_1 - \omega_2^2\delta_2 - \omega_1^2\delta_3 + \omega_1\omega_2\delta_4 , \tag{26}$$

$$4\omega_2\Lambda_2 = \alpha_1 - \omega_1^2(\alpha_2 + \alpha_5) , \tag{27}$$

and $$\omega_1 f_1 = \frac{1}{2} F_1 . \tag{28}$$

Nayfeh, Mook, and Marshall concluded that Λ_1 and Λ_2 have the same sign; otherwise, the unforced ship would be self-oscillating, which is unrealistic due to dissipation.[6]

Substituting equation (17) into equations (24) and (25) and rewriting equation (15) as

$$\varnothing_0 = a_1(T_1)\cos\chi_1, \quad \chi_1 = \omega_1 T_0 + \beta_1(T_1) \tag{29}$$

After seperating real and imaginary parts of equations (24) and (25), using equation(29), and evaluating the terms corresponding to the last term in equation (24) by replacing the function f with $-\mu_3 D_0\varnothing_0 | D_0\varnothing_0 |$. We obtain

$$-\frac{1}{2\pi\omega_1}\int_0^{2\pi}\sin\chi_1 \,(-\mu_3 D_0\varnothing_0 | D_0\varnothing_0 |)d\chi_1 = -\frac{4\mu_3\omega_1}{3\pi} a_1 | a_1 | \tag{30}$$

$$-\frac{1}{2\pi\omega_1}\int_0^{2\pi}\cos\chi_1 \,(-\mu_3 D_0\varnothing_0 | D_0\varnothing_0 |)d\chi_1 = 0 \tag{31}$$

Applying the appropriate transformation of variables, we obtain a generic system of equations as follows:

$$a_1' = -\mu_1 a_1 + a_1 a_2 \sin\gamma_1 + f_1\sin\gamma_2 - \frac{4\mu_3\omega_1}{3\pi} a_1 | a_1 | \tag{32}$$

$$a_2' = -\mu_2 a_2 - a_1^2\sin\gamma_1 \tag{33}$$

$$a_1\beta_1' = -a_1 a_2\cos\gamma_1 - f_1\cos\gamma_2 \tag{34}$$

$$a_2\beta_2' = -a_1^2\cos\gamma_1 \tag{35}$$

where

$$\gamma_1 = \sigma_1 T_1 + \beta_2 - 2\beta_1 \text{ and } \gamma_2 = \sigma_2 T_1 - \beta_1 \tag{36}$$

and the evaluated results given in equations (30) and (31), corresponding to the last term of equation (24), have been used.

4.2 Fixed Points

Periodic solutions of (4) and (5) correspond to the fixed points of equations (32)-(36). They are obtained by setting $a_1' = a_2' = 0$ and $\gamma_1' = \gamma_2' = 0$. It follows from equation (36) that

$$\beta_1' = \sigma_2 \quad \text{and} \quad \beta_2' = 2\sigma_2 - \sigma_1 \tag{37}$$

Hence, the fixed points of equations (32)-(36) are given by the solutions of the following set of coupled nonlinear algebraic equations:

$$\mu_1 a_1 = a_1 a_2 \sin\gamma_1 + f_1 \sin\gamma_2 - \frac{4\mu_3\omega_1}{3\pi} a_1 | a_1 | \quad (38)$$

$$\mu_2 a_2 = -a_1^2 \sin\gamma_1 \quad (39)$$

$$a_1\sigma_2 = -a_1 a_2 \cos\gamma_1 - f_1 \cos\gamma_2 \quad (40)$$

$$(2\sigma_2 - \sigma_1) a_2 = -a_1^2 \cos\gamma_1 \quad (41)$$

Equations (38)-(41) can be manipulated to yield the following polynomial equation for a_1:

$$a_1^6 + d_5 a_1^4 | a_1 | + d_4 a_1^4 + d_3 a_1^2 | a_1 | + d_2 a_1^2 + d_1 | a_1 | + d_0 = 0 \quad (42)$$

where D_i (i=0,1,...,5) are constant coefficents determined from control parameters in use, such as $\sigma_1, \sigma_2, \mu_1, \mu_2, \mu_3, f_1$, and ω_1; they are given by

$$d_0 = -f_1^2 \Gamma_2^2, \quad (43)$$

$$d_1 = 0, \quad (44)$$

$$d_2 = \Gamma_1^2 \Gamma_2^2, \quad (45)$$

$$d_3 = 2\Gamma_2^2 \frac{4\omega_1}{3\pi} \mu_3\mu_1, \quad (46)$$

$$d_4 = 2\mu_1\mu_2 - 2\nu_1\nu_2 + \Gamma_2^2 \left(\frac{4\omega_1}{3\pi} \mu_3 \right)^2, \quad (47)$$

$$d_5 = 2\frac{4\omega_1}{3\pi} \mu_3\mu_2, \quad (48)$$

$$\Gamma_n^2 = \mu_n^2 + \nu_n^2, \quad (49)$$

$$\nu_1 = \sigma_2, \quad (50)$$

and $\nu_2 = 2\sigma_2 - \sigma_1$. (51)

We note that if $\mu_3 = 0$, then $d_3 = d_5 = 0$ and $d_4 = 2\mu_1\mu_2 - 2\nu_1\nu_2$. It follows from equations (38)-(41) that a_2 is given by

$$a_2 = a_1^2 / \Gamma_2 \quad (52)$$

The response in this case is given by

$$\phi = a_1 \cos(\Omega t - \gamma_2) + \ldots \quad (53)$$

$$\theta = a_2 \cos(2\Omega t + \gamma_1 - 2\gamma_2) + \ldots \quad (54)$$

The solutions of the sixth-order algebraic equation (42) are obtained numerically. Then, a_2 is calculated from equation (52). Finally, the corresponding phases γ_1 and γ_2 (β_1 and β_2 also) are obtained from equations (38)-(41).

4.3 Stability of Fixed Points

The stability of the fixed-point solutions are determined by investigating the eigenvalues of the Jacobian matrix of equations (32)-(36).

A given fixed point is asymptotically stable if and only if all the eigenvalues lie in the left half of the complex plane and is unstable if at least one eigenvalue lies in the right half of the complex plane. If a pair of complex-conjugate eigenvalues cross the imaginary axis into the right half of the complex plane with nonzero speed, then we have a Hopf bifurcation. Near these bifurcation points, the response is an amplitude- and phase-modulated combined pitch and roll motion, with the energy being continuously exchanged between the two modes.

5. NUMERICAL RESULTS AND DISCUSSION

5.1 Frequency-Response Curves

The fixed-point solutions are verified by numerically integrating the autonomous amplitude-and phase-modulation equations (32)-(35) using a 5th-and 6th-order Runge-Kutta-Verner algorithm with double precision arithmetics. We examined bifurcations as we vary a bifurcation parameter, such as the detuning parameter σ_2, or the quadratic damping coefficient μ_3 while

all the other parameters ($i.e.$, σ_1, μ_1, μ_2) are kept constant.

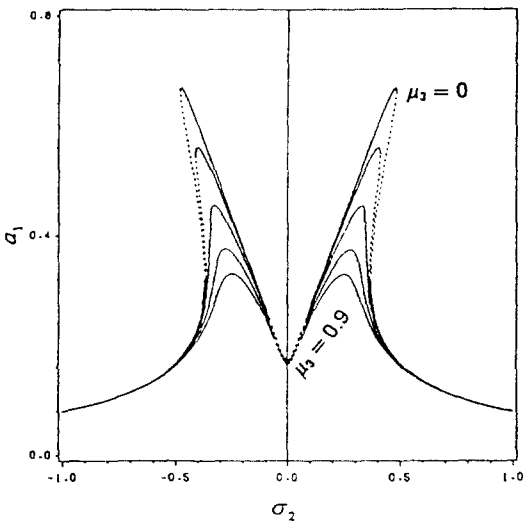

Fig.1 Frequency-Response Curves ($\sigma_1 = 0$): variation of roll amplitude a_1 for different values of μ_3; stable(-), unstable(...)

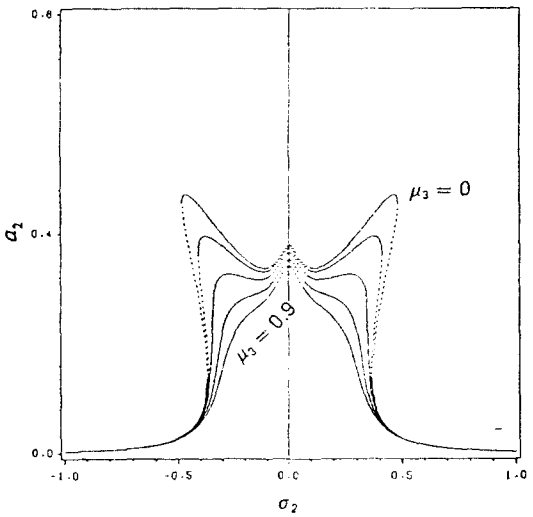

Fig.2 Frequency-Response Curves ($\sigma_1 = 0$): variation of pitch amplitude a_2 for different values of μ_3; stable(-), unstable(...)

In Figures 1 and 2, we show the frequency-response curves when $\mu_1 = \mu_2 = 0.08$, $\sigma_1 = 0$, and $f_1 = 0.08$ for different values of μ_3. The unstable solutions are represented by broken lines and the stable solutions are marked by solid lines. Figures 1 and 2 show variations of the roll amplitude a_1 and pitch amplitude a_2 with σ_2 for different values of μ_3. As μ_3 increases from zero to 0.3, the reversed pitchfork bifurcation points slightly change, whereas the saddle-node bifurcation points move towards $\sigma_2 = 0$. As μ_3 is increased further to 0.6 and 0.9, the saddle-node bifurcation points disappear and the frequency-response curves become single-valued. Consequently, the jump phenomenon and subcritical instability disappear. Moreover, the Hopf bifurcation points approach each other as μ_3 increases. For example, the Hopf bifurcation interval $-0.09995 \leq \sigma_2 \leq 0.09995$ for $\mu_3 = 0$ shrinks gradually to $-0.055 \leq \sigma_2 \leq 0.055$ for $\mu_3 = 0.9$.

We note that for a fixed value of σ_2, a_1 and a_2 decrease as μ_3 increases. The curves of unstable fixed points around the region of perfect tuning, $\sigma_2 = 0$, converge in both modes. The introduction of quadratic damping μ_3, by attaching antirolling devices like bilge keels, causes the region between the two Hopf bifurcation frequencies to shrink. However, it does not eliminate complicated motions completely in this region.

Figures 3 and 4 show the frequency-response curves for the case in which the values of all the parameters are the same as those in Figures 1 and 2 except that $\sigma_1 = 0.2$. In this case, the curves are shifted slightly to the right and the peak amplitudes of the right branches of the roll mode are smaller than those of the left branches.

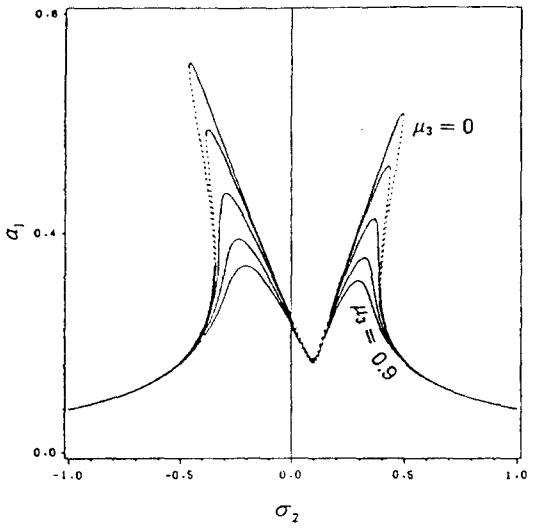

Fig.3 Frequency-Response Curves ($\sigma_1 = 0.2$) : variation of roll amplitude a_1 for different valuse of μ_3 ; stable(-), unstable(...)

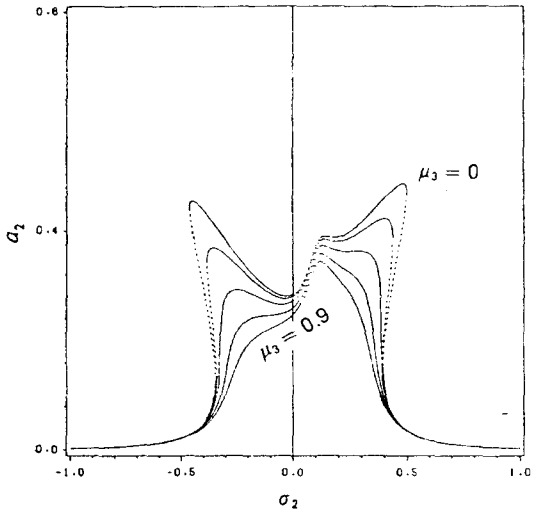

Fig.4 Frequency-Response Curves ($\sigma_1 = 0.2$) : variation of pitch amplitude a_2 for different values of μ_3; stable(-), unstable(...)

The opposite occurs in the response of the pitch mode. If σ_1 is chosen to be negative, the frequency-response curves would be shifted to the left. When $\sigma_1 = 0$, the case of perfect tuning, the curves would be symmetric with respect to $\sigma_2 = 0$. The qualitative behavior of the solutions in the three cases is the same.

5.2 Hopf Bifurcation Region

Figure 5 shows the Hopf bifurcation curves in the parameter space $\sigma_2 - \sigma_1$ for different values of the quadratic damping μ_3 when $-\mu_1 = \mu_2 = 0.02$ and $f_1 = 0.1$. In the outer region, the fixed points of the modulation equations are asymptotically stable and hence correspond to periodic motions. On the transition curves, a complex conjugate pair of eigenvalues of the Jacobian matrix cross the imaginary axis into the right half of the complex plane with nonzero speed. The modulation equations possess limit-cycle solutions near the bifurcation curves. Between the two curves, oscillatory solutions, which may be either limit cycles or chaotic attractors, may be found.

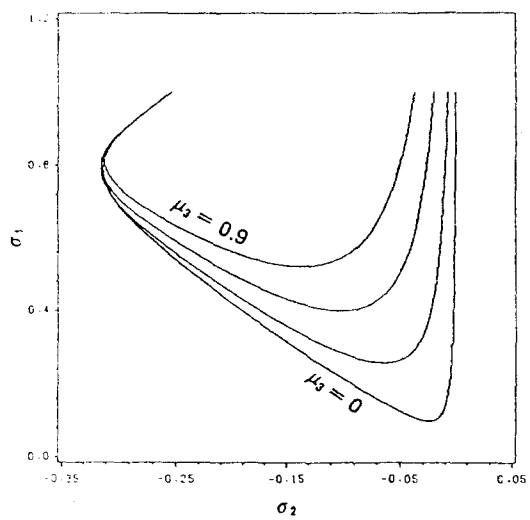

Fig.5 Hopf Bifurcation Curves : for different values of μ_3

Figure 5 shows that the Hopf bifurcation

curves move upward and approach each other as the quadratic roll damping coefficient μ_3 increases. This implies that increasing μ_3 causes the disappearance of aperiodic responses.

6. SUMMARY AND CONCLUSIONS

To design more comfortable and safe vessels, one must understand the complicated dynamics of a vessel moving in a general environment. Included among the important dynamic parameters are the ratios of natural frequencies and the nonlinear interactions among the hydrostatic and hydrodynamic forces and moments. One of the objectives of the present work is to investigate the undesirable and potentially dangerous characteristics of the dynamics of a vessel.

It has been believed for a long time that the linear-plus-quadratic model could adequately describe the hydrodynamic damping of the roll motion. However, many investigators avoided using this model because of the difficulties in the analyses. In the present paper, a quadratic nonlinear damping model is introduced into the equation of the roll mode.

We investigated the nonlinearly coupled pitch and roll response of a vessel in regular waves when the natural frequency in pitch is twice that of roll (a condition of a two-to-one internal or autoparametric resonance). The method of multiple scales was used to derive four first-order autonomous ordinary-differential equations for the modulation of the amplitudes and phases of the pitch and roll modes when either mode is excited. The modulation equations were used to determine the influence of the quadratic nonlinear damping on the periodic responses and their stability.

When the encounter frequency is near the roll natural frequency, the jump phenomenon exists for both zero and nonzero quadratic roll damping. The amplitudes of both the roll mode and the pitch mode decrease as the magnitude of the quadratic roll damping coefficient μ_3 increases. In the frequency-response curves, the overhang regions narrow down as μ_3 increases.

The fixed points of the modulation equations undergo a Hopf bifurcation as one of the control parameters, such as the encounter frequency or excitation amplitude, is varied. Between the Hopf bifurcation points, the response is an amplitude- and phase-modulated motion consisting of both the pitch and roll modes.

REFERENCES

1) Nayfeh, A. H. and Mook, D. T., "Nonlinear Oscillations," Wiley, New York, 1979
2) Froude, W., "Remarks on Mr. Scott-Russell's Paper on Rolling," The papers of William Froude, published by the Institution of Naval Architects, 1995
3) Evan-Iwanowski, R. M., "Resonance Oscillations in Mechanical Systems," Elsevier Scientific Publishing Co., New York, 1976
4) Schmidt, G. and Tondl, A., "Nonlinear Vibrations," Akademie-Verlag, Berlin, 1986
5) Paulling, J. R. and Rosenberg, R. M., "On Unstable Ship Motions Resulting from Nonlinear Coupling," Journal of Ship Research, Vol. 3, p. 36, 1959
6) Nayfeh, A. H. and Mook, D. T., and Marshall, L. R., "Nonlinear Coupling of Pitch and Roll Modes in Ship Motion," Journal of Hydronautics, Vol. 7, p. 145, Oct. 1973
7) Oh, I. G., "Theoretical and Experimental Nonlinear Dynamics of Floating Oscillatory System," Ph. D. Dissertation, Department of Engineering Science and Mechanics, Virginia Polytechnic Institute and State University, Blacksburg, Virginia, 1991